https://doi.org/10.15407/ujpe69.2.96

I. IGNATOV,[1] M.T. ILIEV,[2] T.P. POPOVA,[3] G. GLUHCHEV,[4] P.S. GRAMATIKOV,[5,6] P. VASSILEVA[7]

[1] Scientific Research Center of Medical Biophysics
(32, N. Kopernik Str., Sofia 1111, Bulgaria; e-mail: mbioph@abv.bg)
[2] Faculty of Physics, Sofia University "St. Kliment Ohridski"
(Sofia 1000, Bulgaria)
[3] University of Forestry, Faculty of Veterinary Medicine
(10 Kl. Ohridski Blvd., Sofia 1756, Bulgaria)
[4] Institute of Information and Communication Technologies,
Bulgarian Academy of Sciences (BAS)
(Sofia 1113, Bulgaria)
[5] Department of Green Energetics, European Polytechnical University
(23, Sv. Sv. Kiril i Metodiy Str., Pernik 2300, Bulgaria)
[6] Physics Department, South-West University "Neofit Rilski"
(Blagoevgrad 2700, Bulgaria)
[7] Institute of General and Inorganic Chemistry (IGIC),
Bulgarian Academy of Sciences (BAS)
(Acad. G. Bonchev Street, bl. 11, Sofia 1113, Bulgaria)

METEOROLOGICAL DATA AND SPECTRAL ANALYSES OF NON-EQUILIBRIUM PROCESSES IN WATER DURING THE TOTAL SOLAR ECLIPSE OF 11.08.1999 IN BULGARIA

There are partial or total solar eclipses every year on our planet. They are observed from relatively small areas. From 1950 to 2100, three total solar eclipses fell within the territory of Bulgaria. The two solar eclipses from the 20^{th} century were observed on 15.02.1961 and 11.08.1999. The next total solar eclipse will happen on 3.09.2081. The partial solar eclipses in Bulgaria were on 3.10.2005, 29.03.2006, 1.09.2008, 4.01.2011, and 25.10.2022. The question of the influence of solar eclipses on the Earth's atmosphere, water, and living organisms is an area of interest for many researchers. In this connection, studies have been conducted on atmospheric and water parameters during partial and total solar eclipses. Most investigations were performed with meteorological data – temperature and humidity. In the last 30 years, other methods have also been applied for the investigations of solar eclipses – spectral methods with infrared (IR) spectroscopy, studies of magnetic and electric fields, polarization, and measurements of the parameters of the fluids in plants. Our studies have used meteorological methods and analyses. For the effects on the water, spectral methods are applied to the non-equilibrium energy spectrum (NES) and differential non-equilibrium spectrum (DNES). A deionized water sample examined during the solar eclipse on 11.08.1999 was used, aiming to analyze the parameters of NES and DNES. The deionized water control sample was tested on 10.08.1999 at the same time as the solar eclipse of the next day. The results of our research show relatively rapid and significant changes in air parameters during a solar eclipse, which are most prominent immediately after its culmination. The conditions of non-equilibrium arising during the solar eclipse allow for studying the restructuring of the hydrogen bonds of water molecules. The results of the current studies prove that the solar eclipse's significantly affect water which is the primary substance in the Nature and living organisms. These data are consistent with other ones which also prove that, during a solar eclipse, the structure of water undergoes significant changes. By influencing the water, this natural phenomenon affects the whole Nature and all living organisms on the planet.

K e y w o r d s: solar eclipse, meteorological parameters, NES, DNES.

1. Introduction

Most studies of solar eclipses have been conducted on changes in air temperature and humidity [1, 2].

During the solar eclipses in Bulgaria on 11.08.1999 and 29.06.2006, the brightness of the solar corona [3, 4], gravity wave-like oscillation in the ionosphere [5], as well as spectral parameters [6], were studied.

The researches show that the electromagnetic hydrogen bonds in the water are sensitive to external geophysical and cosmic influences. The action of the solar energy causes the breaking of many hydrogen bonds. This process releases a lot of latent heat [7]. It is established that there is a "window" of transparency in the atmosphere between 8 to 14 μm, in which thermal radiation reaches the Earth from cosmic space and vice versa [8]. The evidence exists that there are variations in thermal radiation under clear skies. Such variations are related to water vapor due to the variable atmospheric concentration of water dimers linked by weak hydrogen bonds [9].

Effects are established on the weaker hydrogen bonds at a light wavelength (λ) between 8 to 14 μm [9–11].

At λ from 8 to 14 μm and $\tilde{v}$ from 1250 to 714 cm^{-1}, the highest level of the polarization of infrared radiation is observed in the absorption and reflection of water ($\sim$4–10%) [12].

Dang analyzed polarization effects in modeling a hydrogen bond in water using classical molecular dynamics techniques [13].

During the solar eclipses, the anomalies of magnetic fields and the near-surface atmospheric electricity are recorded [14–16].

Non-equilibrium processes were described in the atmosphere and water with spectral methods. Non-equilibrium energy spectrum (NES) and Differential non-equilibrium energy spectrum (DNES) were considered in [10, 17]. The spectral methods NES and DNES are suitable for applications when studying the hydrogen bonds among water molecules due to various influences from the environment and the cosmic space [10, 18–20].

Of interest are the studies of the effects of the solar eclipse on 11.08.1999 on the parameters of fluids in trees. Through the entropy analysis, it was proved that the energy of hydrogen bonds among water molecules increases [21].

The analyses of the parameters of binary clusters of water molecules, as in solar eclipses [9], provide information on environmental impacts and chemical processes. 2 and 3-molecule clusters are found on the Mars in the subsurface lake with water. There is the evidence of that water clusters take part in the formation of amino acid glycine $C_2H_5NO_2$ in Martian water [22]. The research was conducted in the Interstellar Medium (ISM) to structure glycine. The model involves a binary structure of two water molecules, H_2O–H_2O, $CH_2=NH$, and CO [23].

2. Methods and Materials

2.1. Water samples

The deionized water samples were used and examined during the solar eclipse on 11.08.1999 aiming to analyze the parameters of NES and DNES. The deionized water control samples were tested on 10.08.1999 at the same time as the solar eclipse of the next day.

2.2. The analysis of NES and DNES

The wetting angle θ was measured with a specially designed instrument. Evaporation of deionized water drops was performed in a sealed chamber with a stable temperature of 22 °C [24–26] (Fig. 1). The drops were placed on a 350 μm thick BoPET (biaxially oriented polyethylene terephthalate) sheet. The device has the following technical features:

- monochromatic filter with the wavelength $\lambda = 580 \pm 7$ nm;
- water evaporation angle ranging from 72.3 deg to 0 deg;
- the measured range of the energy of hydrogen bonds among water molecules is $\lambda = 8.9$–13.8 μm or $E = -0.08 - -0.1387$ eV [27, 28].

Luck considered that water consists of hydrogen bonds between one water molecule's hydrogen atom and another's oxygen [29]. Most of them are bound

Citation: Ignatov I, Iliev M.T., Popova T.P., Gluhchev G., Gramatikov P.S., Vassileva P. Meteorological data and spectral analyses of non-equilibrium processes in water during the total solar eclipse of 11.08.1999 in Bulgaria. *Ukr. J. Phys.* **69**, No. 2, 96 (2024). https://doi.org/10.15407/ujpe69.2.96.
Цитування: Ігнатов І., Ілієв М.Т., Попова Т.П., Глухчев Г., Граматіков П.С., Вассілева П. Метеорологічні дані та спектральний аналіз нерівноважних процесів у воді протягом повного сонячного затемнення, яке спостерігалося 11.08.1999 р. у Болгарії. *Укр. фіз. журн.* **69**, №2, 96 (2024).

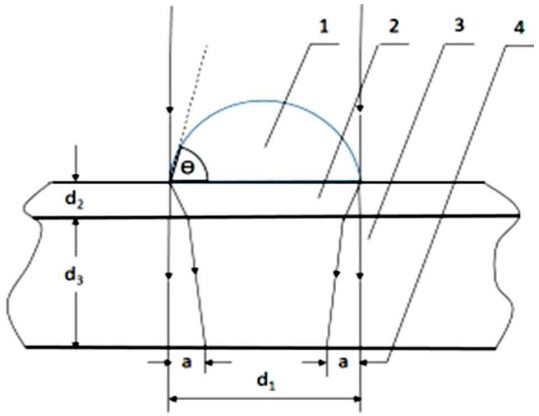

Fig. 1. Operating principle of the method for measuring the wetting angle of liquid drops on a hard surface: drop (*1*), thin mylar sheet (*2*), glass plate (*3*), refraction ring width (*4*). The wetting angle θ is a function of $\mathbf{a}$ and $\mathbf{d}_1$

by the energy of the connection ($-E$), and the remaining are free ($E = 0$). It is accepted that E has a negative value. This is known as the Luck two-state model [30]. The number of hydrogen bonds between the hydrogen atom of one water molecule and the oxygen of another one in a particular volume of water is twice as high as the number of molecules it contains.

A part of the hydrogen bonds is restructured in a proximity of the spherical part of the drop surface [31]. As a result, we obtain the dependence between the surface tension δ and the hydrogen bond energy [32–34]:

$$\delta = -kT\, I\, \ln[1 + \alpha/[\exp(-\beta E) + \alpha]. \tag{1}$$

Here, k is the Boltzmann constant, $\beta = 1/kT$, T is the absolute temperature, E is the hydrogen bond energy, α is the ratio of two subvolumes of the phase space related to the structuring and restructuring of hydrogen bonds, $\alpha = 28 \pm 8$, and $I = 5.03 \times 10^{18}$ m^{-2} is the density of water molecules in the hydrophobic surface layer.

The values of E and α are determined by comparison with the experiment. Expression (1) explains the fraction C of the actual surface tension γ, i.e., $\delta d = C\gamma$ [35, 36]. According to [36], the contribution of the non-hydrogen bond interaction amounts to 20% of the real value of γ and $C = 4/5$.

Consider the Helmholtz free surface energy $F = \gamma\Sigma$, where Σ is the spherical part of the drop surface [18].

At the instant of mechanical equilibrium, F should be minimal, i.e., $dF = 0 = d(\gamma\Sigma)$ [18]

$$0 = \gamma\Sigma - \gamma_0\Sigma_0. \tag{2}$$

The evaporation process of water drops occurs at a constant temperature of 20 °C in a hermetic camera [26].

The expressions for Σ_0 and Σ are as follows [18]:

$$\Sigma = \pi D^2/2(1 + \cos\,\theta); \quad \Sigma_0 = \pi D^2/2(1 + \cos\theta_0), \tag{3}$$

$$-E/kT = C\gamma/I\,kT, \tag{4}$$

$$E = C\gamma o(1 + \cos\,\theta)/I(1 + \cos\theta_0). \tag{5}$$

During the process, the wetting angle changes in discrete steps and characterizes the average energy of hydrogen bonds as follows:

$$\theta = \arccos(-1 + bE), \quad b = I(1 + \cos\theta_0)/C\gamma o, \tag{6}$$

where θ is the wetting angle, E is the average energy of hydrogen bonds, and b is a temperature-dependent parameter [37, 38]. The development of the method involves the non-equilibrium energy spectrum (NES) and differential non-equilibrium spectrum (DNES) [39]. They are used to research natural waters [40, 41] and osmosis [42]. The molecular dynamics simulation is applied to investigate the wetting behavior of water droplets on the sandstone surface under different salinities. The equilibrium configuration of the system was used to study the interaction of its components. The number of hydrogen bonds was calculated in [43].

The energy (E) of hydrogen bonds among H_2O molecules in water samples is measured in eV. The function $f(E)$ is called the energy distribution spectrum. The non-equilibrium evaporation process of water droplets characterizes the energy spectrum of water. This non-equilibrium energy spectrum (NES) is measured in eV^{-1}. DNES is defined as the difference [10, 43, 44]:

$$\Delta f(E) = f(\text{water sample}) - f(\text{control water sample}). \tag{7}$$

DNES is measured in eV^{-1}, where $f(*)$ denotes the evaluated energy [18, 43].

3. Results

Figure 2 illustrates the full solar eclipse on 11.08.1999.

3.1. Meteorological data

Table 1 shows the visible movement of the Sun and the Moon in Sofia, Bulgaria (official time). The solar eclipse's impact was studied, which in its maximum phase was 94.4% on the daily course of the meteorological parameters.

On the eclipse day, the moon transitioned from its last quarter to the new moon phase at 14:09 on 11.08.2023. Figure 3 shows the air temperature (t °C) as a function of time (time of day – h).

The graph indicates the drop in the air temperature by more than 5 °C in the hour immediately after the culmination of the solar eclipse, followed by an increase within the norm in the following hours.

Figure 4 shows the relative humidity (RH, %) as a function of the time (time of day – h). As the chart shows, this indicator rises by over 10% within 1 hour after the eclipse's culmination.

Figures 5 and 6 present the results of more frequent measurements of the temperature and the air's relative humidity around the eclipse's total phase.

Fig. 2. Full solar eclipse on 11.08.1999

Table 1. **Impact of the solar eclipse with maximum phase 94.4% on the daily course of meteorological parameters**

Daily course of 11.08.1999	Sun	Moon
Sunrise	06.28 h	06.11 h
Upper culmination	13.32 h	13.31 h
Sunset	20.35 h	20.43 h

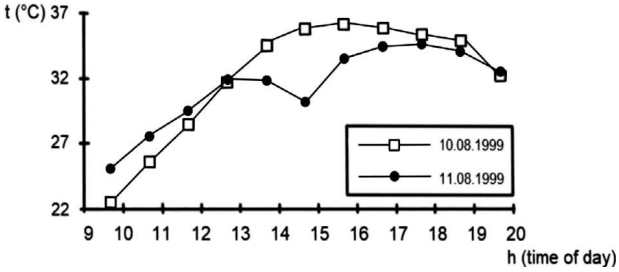

Fig. 3. Air temperature as a function of time

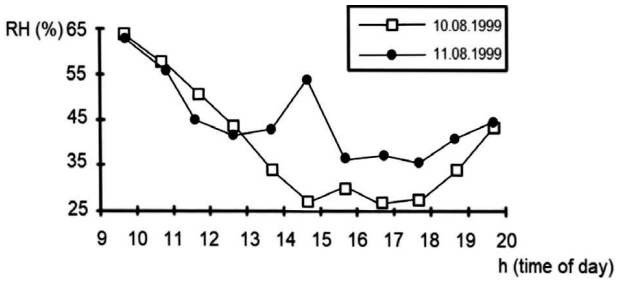

Fig. 4. Relative humidity as a function of the time

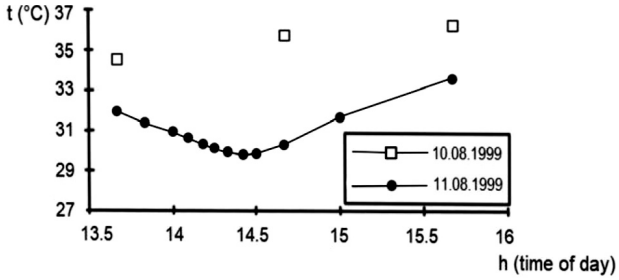

Fig. 5. Alterations in the air temperature around the total phase of the eclipse

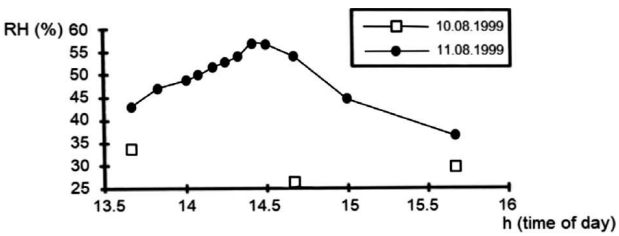

Fig. 6. Changes in the relative air humidity around the total phase of the eclipse

Table 2. **The distribution function for energies $f(E)$ in eV^{-1} according to the value of $(-E)$ of hydrogen bonds**

$-E$ (eV) x-axis	Deionized water solar eclipse $f(E)$ (eV^{-1})	Deionized water control sample $f(E)$ (eV^{-1})	$-E$ (eV) x-axis	Deionized water solar eclipse $f(E)$ (eV^{-1})	Deionized water control sample $f(E)$ (eV^{-1})
0.0937	0	30.1	0.1187	15.1	0
0.0962	23.1	0	0.1212	30.2	30.2
0.0987	23.1	38.5	0.1237	0	15.1
0.1012	0	46.2	0.1262	15.1	30.2
0.1037	30.2	38.5	0.1287	15.1	30.2
0.1062	0	30.2	0.1312	30.1	23.1
0.1087	15.1	46.2	0.1337	15.1	23.1
0.1112	46.2	0	0.1362	46.2	0
0.1137	15.1	23.1	0.1387	76.9	0
0.1162	0	23.1	–	–	–

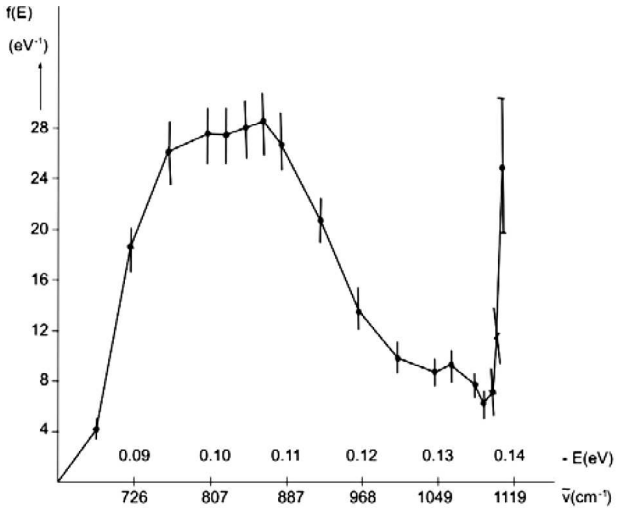

Fig. 7. NES of 39 independent measurements in one year

Fig. 8. Sunglasses for the public observation of the solar eclipse on 11.08.1999

From the results presented in the figures, it can be clearly seen that, till the beginning of the eclipse, which is one hour before the upper culmination of the Sun, there is no change in the daily meteorological course of the meteorological parameters. The air temperature shows a linear increase, while the relative humidity shows a linear decrease. During the previous day, 10.08.1999, a "plateau" was observed from 14:00 to 18:00 h. The maximum temperature value $t_{\max} = 36.3$ °C falls between 15:00 and 16:00 h. The relative humidity between 15:00 and 16:00 h has a minimum value of $\mathrm{RH}_{\max} = 27\%$. Before the beginning of the solar eclipse on 11^{th} August, due to the reduced solar radiation, there is a change in the daily course of the meteorological elements. During the eclipse, the air temperature goes through a minimum min = 29.7 °C, and the relative humidity goes through a maximum of $\mathrm{RH}_{\max} = 27\%$.

The wind at the eclipse is up to 1 $\mathrm{m \cdot s^{-1}}$. During the natural phenomenon, the atmospheric pressure decreases. Such a barometric trend is typical of a solar eclipse; immediately after the total solar eclipse, 3 to 10 mid-level cumulus clouds developed at an altitude of 2000 to 4000 m. Afterward, the weather got sunny again. The interference and diffraction patterns were registered in the zone of totality.

3.2. Spectral methods NES and DNES

Within the method, we performed 39 independent measurements in one year, by using NES. The average value of the energy among the water molecules

was determined with the value $E = -1090$ eV or $\lambda = 11.38$ μm, $\tilde{v} = 879$ cm^{-1} (Fig. 7) [10]. According to the Student's t-test $p < 0.001$, the statistical data have the correlation coefficient $r = 0.54$.

For each sample during a solar eclipse on 11.08.1999, 10 measurements of deionized water were performed. On 10.08.1999, 10 measurements were made on the control samples with deionized water at the same time as the solar eclipse time. Student's t-test was applied.

There was a statistically significant difference between the three groups of results with the samples and control samples according to the Student's t-test at the $p < 0.001$ level with the correlation coefficient $r = 0.0265$. The average results are: $\mathrm{NES}_{\mathrm{sample}} = -0.1213$ eV, $\mathrm{NES}_{\mathrm{control\,sample}} = -0.1175$ eV, $\mathrm{DNES} = -0.0038$ eV.

Table 2 illustrates the distribution function for energies $f(E)$ in eV^{-1} according to the value of $(-E)$ of hydrogen bonds [17].

The study shows an increase in the surface tension of water during the solar eclipse [45]. The result of our research on the surface tension for the solar eclipse on 11.08.1999 is $\gamma = 0.072$ J $\cdot$ m^{-2} and on 10.08.1999 is $\gamma = 0.068$ J $\cdot$ m^{-2}.

One of the main reasons for the alteration of water's surface tension during the solar eclipse is the disputed effect of an eclipse on the ozone (O_3) layer.

Several studies claim that the solar eclipses impact Earth's ozone layer [46, 47].

The isotopic ratio in CO_2 and the carbon dioxide mixing ratio in the air samples collected during the event differ from neighboring samples, suggesting the role of atmospheric inversion in trapping the emitted CO_2 from the urban atmosphere during the solar eclipse [48].

The behavior of surface ozone and nitrogen dioxide (NO_2) concentration, as well as the variations in various meteorological parameters before, during, and after the total solar eclipse of 29 March 2006, has been examined [48, 49]. The studies show the changes in the compounds in the atmosphere during the solar eclipse – ozone (O_3) layer, carbon dioxide (CO_2), and nitrogen dioxide (NO_2). The results illustrate the possibility for changes in the Earth's atmosphere during phenomena such as solar eclipses and connected effects on water. Figure 8 illustrates the sunglasses for the public observation of the solar eclipse on 11.08.1999.

4. Conclusions

The results of our research show relatively rapid and significant changes in air parameters during a solar eclipse, which are most prominent immediately after its culmination. While the temperature decreases due to a reduction in the strength of solar radiation, the humidity increases, which can also explain a reduction of sunshine and temperature change. The formation of cumulus clouds at the same time also confirms the considerable change in atmospheric parameters of the compounds such as the ozone (O_3) layer, carbon dioxide (CO_2), and nitrogen dioxide (NO_2) under the influence of the eclipse.

The conditions of non-equilibrium arising during a solar eclipse allow one to study the restructuring of hydrogen bonds between water molecules.

Water is the main substance of living organisms. We have proven that, during a solar eclipse, the structure of water undergoes significant changes. By influencing the water, this natural phenomenon affects the whole Nature and all living organisms on the planet. The research results are helpful for the effects on cosmic expeditions and staying on the Moon, Mars, and other planets under non-equilibrium conditions. The non-equilibrium can result from electromagnetic and gravitation fields and different atmospheric changes with temperature differences.

The authors thank Kiril Avramov and Emil Stoimenov for the meteorological research they performed.

The article is in the memory of Prof. Anton Antonov (1934–2021).

1. P. Krishnan, P.K. Kunhikrishnan, S.M. Nair *et al.* Observations of the atmospheric surface layer parameters over a semi-arid region during the solar eclipse of August 11$^{\mathrm{th}}$, 1999. *J. Earth System Sci.* **113**, 353 (2004).
2. B. Paramitha, R. Zaen, A.B.D. Nandiyanto. Changes in meteorological parameters (i.e. UV and solar radiation, air temperature, humidity, and wind condition) during the partial solar eclipse of 9 March 2016. *IOP Conf. Ser.: Mater. Sci. Eng.* **180**, 012131 (2017).
3. B.A. Marzouk, P. Stoeva, A. Stoev. White light coronal structure and flattening during six total solar eclipses. *NRIAG J. Astron. Geophys.* **297** (2016).
4. A. Stoev, P. Stoeva, S. Kuzin *et al.* Processing methods and approaches for the analysis of images of the eclipsed solar corona taken during campaigns with the participation of amateur astronomers. *Proc. Int. Astron. Union* **15**, 365 (2019).

5. D. Altadill, J.G. Sole, E.M. Apostolov. Vertical structure of a gravity wave-like oscillation in the ionosphere generated by the solar eclipse of August 11, 1999. *JGR Space Physics* **106**, 21419 (2001).
6. D.D. Krezhova, A.H. Krumov, T.K. Yanev. Spectral investigations of the solar radiation during the total solar eclipse on March 29, 2006. *J. Atmos Sol. Terr. Phys.* **70**, 365 (2008).
7. F. Zhao, Y. Guo, X. Zhou *et al.* Materials for solar-powered water evaporation. *Nat. Rev. Mater.* **5**, 388 (2020).
8. Sh.B. Ilso. A set of equations for full spectrum and 8- to 14-μm and 10.5- to 12.5-μm thermal radiation from cloudless skies. *Water Resour. Res.* **17**, 295 (1981).
9. V. Vaida, J.S. Daniel, H.G. Kjaergaard *et al.* Atmospheric absorption of near-infrared and visible solar radiation by the hydrogen-bonded water dimer. *QJR Meteorol Soc.* **127**, 1627 (2001).
10. A. Antonov. Research of the non-equilibrium processes in the area in allocated systems. *DSc Thesis*, *Southwest University Neofit Rilski, Blagoevgrad, Bulgaria* 1 (1995) [in Bulgarian].
11. I. Ignatov, H. Niggli, Ch. Drossinakis *et al.* Methods for registering non-ionizing radiation emitted from the human body. *Europ. Rev. Chem. Res.* **3**, 4 (2015).
12. J.A. Shaw. Degree of linear polarization in spectral radiances from water-viewing infrared radiometers. *Applied Optics* **38**, 315 (1999).
13. X.L. Dang. Importance of polarization effects in modeling the hydrogen bond in water using classical molecular dynamics techniques. *J. Phys. Chem. B* **102**, 620 (1998).
14. A.J. Bennett. Effects of the March 2015 solar eclipse on near-surface atmospheric electricity. *Phil. Trans. R. Soc. A* **374**, 20150215 (2016).
15. B. Heilig, A. Csontos, P. Kovacs. The geomagnetic effect of the solar eclipse of 11 August 1999. *Contrib. Geophys. Geod.* **31**, 323 (2001).
16. L. Chernogor. Geomagnetic effect of the solar eclipse of June 10, 2021. *Kinemat. Phys. Celest. Bodies.* **38**, 11 (2022).
17. I. Ignatov, M.T. Iliev, P. Gramatikov *et al.* Non-equilibrium processes in the atmosphere, water, and reactions with calcium carbonate in the environment. *J. Chem. Technol. Metall.* **58**, 1100 (2023).
18. L. Todorova, A. Antonov. Note on the drop evaporation method for studying water hydrogen bond distribution: I. A filtration application. *C. R. Acad. Bulg. Sci.* **53**, 7 (2000).
19. S. Todorov, A. Damianova, A. Antonov *et al.* Water energy spectrum method and Investigation of the variations of the H-bond structure of natural waters. *C. R. Acad. Bulg. Sci.* **61**, 857 (2008).
20. I. Ignatov, N. Valcheva. Physicochemical, isotopic, spectral, and microbiological analyses of water from glacier Mappa, Chilean Andes. *J. Chil. Chem. Soc.* **68**, 5802 (2023).
21. H. Tributsch, J. Cermak, N. Nadezhdina. Kinetic studies on the tensile state of water in trees. *J. Phys. Chem. B* **109**, 17693 (2003).
22. H. Laurent. A. Soper, L. Dougan. Biomolecular self-assembly under extreme Martian mimetic conditions. *Mol. Phys.* **117** (22), 3398 (2019).
23. Z.P. Nhlabatsi, P. Bhasi, S. Sitha. Possible interstellar formation of glycine from the reaction of CH_2 =NH, CO, and H_2O: Catalysis by extra water molecules through the hydrogen relay transport. *Phys. Chem. Chem. Phys.* **18**, 375 (2016).
24. I. Ignatov, G. Gluhchev, N. Neshev, D. Mehandjiev. Structuring of water clusters depending on the energy of hydrogen bonds in electrochemically activated waters Anolyte and Catholyte. *Bulg. Chem. Commun.* **53**, 234 (2021).
25. A. Antonov, L. Yuskesselieva. Method for determination of structural changes in Liquids. *Author's certificate of the invention* 43821 (1983).
26. A. Antonov. An optical method version for determination of the welling angle of liquids. *C. R. Acad. Bulg. Sci.* **37**, 1199 (1984).
27. A. Antonov, L. Yuskesselieva, I. Teodossieva. Influence of ions on the structure of water under conditions far away from equilibrium. *Physiologie.* **26**, 2552 (1989).
28. P. Gramatikov, A. Antonov. On the two conditions model of water structure. *C. R. Acad. Bulg. Sci.* **50**, 13 (1997).
29. W. Luck. A model of hydrogen-bonded liquids. *Angewandte Chemie.* **19**, 28 (1980).
30. G. Kontogeorgis, M.A. Hoster, A.N. Kottaki *et al.* Water structure, properties and some applications – a review. *Chem. Thermodyn. Thermal Anal.* **6**, 100053 (2022).
31. L.F. Vega, F. Lovel. Review and new insights into the application of molecular-based equation of state to water and aqueous solutions. *Fluid Ph. Equilib.* **416**, 150 (2016).
32. I. Ignatov, M.T. Iliev, P.S. Gramatikov. Education program on physics and chemistry for non-equilibrium processes at the interfaces between solid-liquid-gaseous media. *Eur. J. Contemp. Educ.* **12** (3), 862 (2023).
33. S. Aparicio-Martínez, K. Hall. Phase equilibria in water containing binary systems from molecular-based equations of state. *Fluid Phase Equilib.* **254**, 112 (2007).
34. G. Clark, A. Haslam, A. Galindo, G. Jackson. Developing optimal Wertheim – like models of water for use in statistical associating fluid theory (SAFT) and related approaches. *Mol. Phys.* **104**, 3561 (2010).
35. B.J. Zhang, J. Kim, T.Ch. Lee. Behavior of an evaporating water droplet on a lubricant-impregnated nano-structured surface. *Exp. Therm. Fluid Sci.* **96**, 216 (2018).
36. A. Luzar, S. Svetina, B. Žekš. The contribution of hydrogen bonds to the surface tension of water. *Chem. Phys. Lett.* **96**, 485 (1983).
37. A.C. Kumbharkhane, Y.S. Joshi, S.C. Mehrotra *et al.* Study of hydrogen bonding and thermodynamic behavior in water–1,4-dioxane mixture using time domain reflectometry. *Physic B: Condensed Matter.* **421**, 1 (2013).
38. P. Gramatikov, A. Antonov, M. Gramatikova. Study of the properties and structure variations of water systems under the stimulus of outside influences. *Fresenius J. Anal. Chem.* **343**, 134 (1992).

39. A.S. Antonov, T.D. Galabova, G.J. Jelev, J.G. Jelev. New technology for recording the information based on intramolecular bonds in water. In: *Proceedings of the International Spring Seminar on Electronics Technology* **3** (569–573), 1490880 (2004).
40. S. Todorov, A. Damianova, A. Antonov, L. Todorova. Investigations of natural waters spectra from the lakes of Rila Mountain National Park. *C. R. Acad. Bulg. Sci.* **63**, 555 (2010).
41. S. Boteva, A. Kenarova, G. Radeva *et al.* Community dynamics of pelagic bacteria in the high mountain lake Bubreka, Rila mountain. Bulgaria. *Biotechnol. Biotechnol. Equip.* **25** (4), 2620 (2014).
42. D. Mehandjiev, I. Ignatov, N. Neshev *et al.* History-dependent hydrogen bonds energy distributions in NaCl aqueous solutions undergoing osmosis and diffusion through a ceramic barrier. *J. Chem. Technol. Metall.* **58**, 340 (2023).
43. I. Ignatov, F. Huether, N. Neshev *et al.* Research of water molecules cluster structuring during *Haberlea rhodopensis* Friv. hydration. *Plants*, **11**, i2655 (2022).
44. M.T. Iliev, F. Huether, I. Ignatov, P.S. Gramatikov. Education of students on Physics and Chemistry with effects of water filtration. Modeling of water clusters and hexagonal structures. *Eur. J. Contemp. Educ.* **12**, 1546 (2023).
45. E.C. Fuchs, G. Oudakker, M. Justinek *et al.* Solar eclipses and the surface properties of water. *Earth Moon Planets.* **123**, 15 (2019).
46. S. Zerefos, D.S. Balis, P. Zanis *et al.* Changes in surface UV solar irradiance and ozone over the Balkans during the eclipse of Aug 11, 1999. *Adv. Space Res.* **27**, 1955 (2001).
47. Y. Tian, J. Li, Ch. Yang. Effects of the annular eclipse on the surface O_3 in Yunnan province. *China. Front. Environ. Sci.* **10**, 968507 (2022).
48. T. Guha, P. Ghosh. An experimental set-up for carbon isotopic analysis of atmospheric CO_2 and an example of ecosystem response during solar eclipse 2010. *J Earth Syst Sci.* **122**, 623 (2013).
49. C. Tzanis, C. Varotos, L. Viras. Impacts of the solar eclipse of 29 March 2006 on the surface ozone and nitrogen dioxide concentrations at Athens, Greece. *Atmos. Chem. Phys. Discuss.* **7**, 14331 (2007).

Received 20.01.24

І. Ігнатов, М.Т. Іліев, Т.П. Попова,
Г. Глухчев, П.С. Граматіков, П. Вассілева

МЕТЕОРОЛОГІЧНІ ДАНІ ТА СПЕКТРАЛЬНИЙ АНАЛІЗ НЕРІВНОВАЖНИХ ПРОЦЕСІВ У ВОДІ ПРОТЯГОМ ПОВНОГО СОНЯЧНОГО ЗАТЕМНЕННЯ, ЯКЕ СПОСТЕРІГАЛОСЯ 11.08.1999 р. У БОЛГАРІЇ

Використано метеорологічні дані щодо температури і вологості повітря та застосовано спектральні методи для дослідження нерівноважних енергетичних спектрів зразків деіонізованої води. Знайдено відносно швидкі значні зміни параметрів повітря протягом сонячного затемнення. Показано, що нерівноважність процесів протягом сонячного затемнення веде до змін у структурі водневих зв'язків молекул води. Наші результати свідчать про те, що сонячні затемнення суттєво впливають на структуру води, яка є надзвичайно важливою частиною природи і всього живого, і узгоджуються із результатами інших робіт.

Ключові слова: сонячне затемнення, метеорологічні параметри, нерівноважний енергетичний спектр, диференціальний нерівноважний енергетичний спектр.